



HAL
open science

Molecular Tension Microscopy of E-Cadherin During Epithelial- Mesenchymal Transition

Helena Canever, Pietro Salvatore Carollo, Romain Fleurisson, Philippe Girard, Nicolas Borghi

► **To cite this version:**

Helena Canever, Pietro Salvatore Carollo, Romain Fleurisson, Philippe Girard, Nicolas Borghi. Molecular Tension Microscopy of E-Cadherin During Epithelial- Mesenchymal Transition. The Epithelial-to Mesenchymal Transition, 2021. hal-02989319

HAL Id: hal-02989319

<https://hal.science/hal-02989319>

Submitted on 5 Nov 2020

HAL is a multi-disciplinary open access archive for the deposit and dissemination of scientific research documents, whether they are published or not. The documents may come from teaching and research institutions in France or abroad, or from public or private research centers.

L'archive ouverte pluridisciplinaire **HAL**, est destinée au dépôt et à la diffusion de documents scientifiques de niveau recherche, publiés ou non, émanant des établissements d'enseignement et de recherche français ou étrangers, des laboratoires publics ou privés.

Metadata of the chapter that will be visualized online

Chapter Title	Molecular Tension Microscopy of E-Cadherin During Epithelial-Mesenchymal Transition
---------------	---

Copyright Year	2020
----------------	------

Copyright Holder	Springer Science+Business Media, LLC, part of Springer Nature
------------------	---

Author	Family Name Canever
	Particle
	Given Name Helena
	Suffix
	Division Institut Jacques Monod, CNRS UMR7592
	Organization Université de Paris
	Address Paris, France

Author	Family Name Carollo
	Particle
	Given Name Pietro Salvatore
	Suffix
	Division Institut Jacques Monod, CNRS UMR7592
	Organization Université de Paris
	Address Paris, France

Author	Family Name Fleurisson
	Particle
	Given Name Romain
	Suffix
	Division Institut Jacques Monod, CNRS UMR7592
	Organization Université de Paris
	Address Paris, France

Author	Family Name Girard
	Particle
	Given Name Philippe P.
	Suffix
	Division Institut Jacques Monod, CNRS UMR7592
	Organization Université de Paris
	Address Paris, France
	Division Faculty of Basic and Biomedical Sciences
	Organization Université Paris Descartes
	Address Paris, France

Corresponding Author	Family Name Borghi
	Particle

Given Name **Nicolas**
Suffix
Division Institut Jacques Monod, CNRS UMR7592
Organization Université de Paris
Address Paris, France
Email nicolas.borghi@ijm.fr

Abstract Molecular Tension Microscopy has been increasingly used in the last years to investigate mechanical forces acting in cells at the molecular scale. Here, we describe a protocol to image the tension of the junctional protein E-cadherin in cultured epithelial cells undergoing Epithelial-Mesenchymal Transition (EMT). We report how to prepare cells and induce EMT, and how to acquire, analyze, and quantitatively interpret FRET data.

Keywords FRET Biosensor - E-cadherin - EMT - Microscopy - Mechanotransduction
(separated by '-')

Molecular Tension Microscopy of E-Cadherin During Epithelial-Mesenchymal Transition 2 3

Helena Canever, Pietro Salvatore Carollo, Romain Fleurisson, 4
Philippe P. Girard, and Nicolas Borghi 5

Abstract 6

Molecular Tension Microscopy has been increasingly used in the last years to investigate mechanical forces 7
acting in cells at the molecular scale. Here, we describe a protocol to image the tension of the junctional 8
protein E-cadherin in cultured epithelial cells undergoing Epithelial-Mesenchymal Transition (EMT). We 9
report how to prepare cells and induce EMT, and how to acquire, analyze, and quantitatively interpret 10
FRET data. 11

Key words FRET Biosensor, E-cadherin, EMT, Microscopy, Mechanotransduction 12

1 Introduction 13

Molecular Tension Microscopy (MTM) is the microscopy of molec- 14
ular tension sensors [1]. Molecular tension sensors are a class of 15
Förster Resonance Energy Transfer (FRET) sensors that are sensi- 16
tive to molecular tension. They consist in a FRET pair of fluoro- 17
phores separated by an elastic linker. When a force is exerted on the 18
sensor, the rate of FRET, which is sensitive to the distance and 19
orientation between the donor and acceptor fluorophores, 20
decreases. Knowledge of the relationship between a measure of 21
FRET and the force, from in vitro calibration, allows for the deter- 22
mination of molecular tension [2]. When inserted in a protein of 23
interest, such a sensor can report its tension in live cells. 24

Molecular tension sensors have been in use for nearly 10 years 25
[3]. A variety of sensors with specific operating ranges have been 26
designed [4, 5], and have been used to measure tension in matrix, 27
cytoskeleton, adhesion, glycocalyx, kinetochore, membrane- 28
cytoskeleton linker or motor proteins [2, 3, 6–9] in cultured cells, 29
C. elegans, *Xenopus*, Zebrafish, or *Drosophila* [3, 10–12]. 30

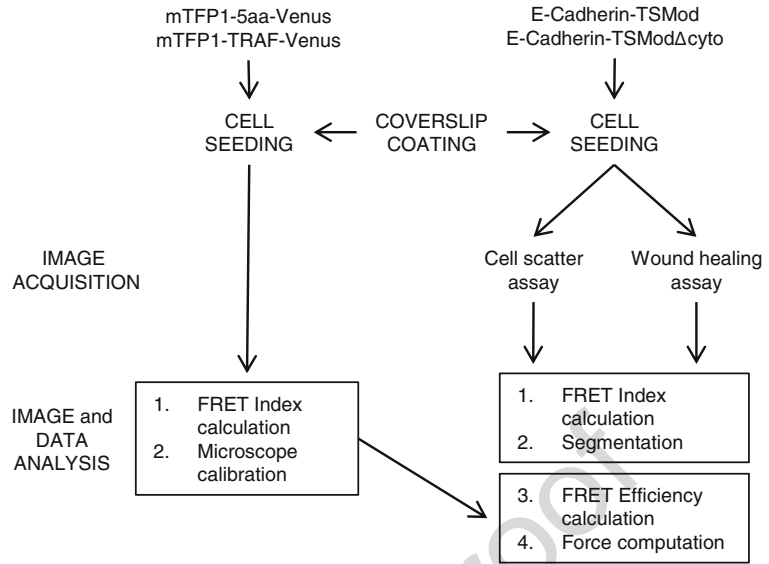


Fig. 1 Experimental workflow for MDCK type II cells sample preparation, EMT induction, image acquisition and image and data analysis

Here, we present a protocol to perform MTM of intercellular adhesion proteins E-cadherins [13] that experience cytoskeleton-generated tension sensitive to external cues [14]. During Epithelial-Mesenchymal Transition (EMT), E-cadherin tension relaxes, which associates with the release of its interactant β -catenin and activation of β -catenin dependent transcription [15].

The protocol describes how to culture epithelial cells (MDCK) stably expressing an E-cadherin tension sensor (E-cadherin-TSMod), induce EMT, and acquire and analyze FRET data using standard confocal microscopy and free image analysis software [16] (see Fig. 1). The protocol may be adapted to other proteins or model systems, on different microscopes as well. General considerations about MTM, its strengths and limitations can be found elsewhere [1].

2 Materials

Store DMEM (Dulbecco's Modified Eagle Medium), trypsin, Dulbecco's Phosphate Buffered Saline (DPBS, that is without Calcium and Magnesium), collagen at 4 °C. Store Foetal Bovine Serum (FBS), Penicillin, Streptomycin, and Hepatocyte Growth Factor (HGF) solution at -80 °C.

2.1 Cell Culture

1. Culture medium: low glucose DMEM with phenol red supplemented with 10% v/v Foetal Bovine Serum (FBS) and Penicillin 10 U/mL + Streptomycin 10 μ g/mL.

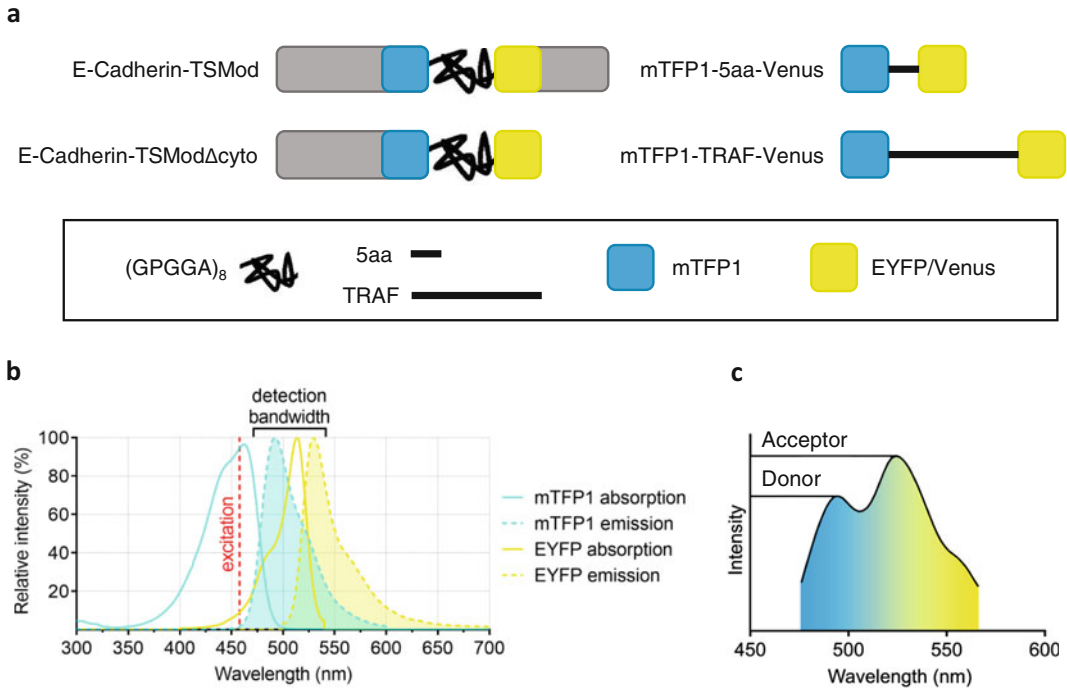


Fig. 2 (a) E-Cadherin-TSMMod, tension-less control E-Cadherin-TSMMod Δ cyto, and high and low FRET calibration constructs. Blue squares represent the donor fluorophore mTFP1, yellow squares represent the acceptor fluorophore EYFP/Venus. Linkers (GPGGA) $_8$, 5aa, and TRAF are represented in black. **(b)** Absorption and emission spectra of mTFP1 and EYFP/Venus. Laser excitation wavelength is indicated by the red dashed line. **(c)** Spectral emission in the detection bandwidth for mTFP1 and EYFP. Donor and acceptor emission peaks are indicated

2. Washing medium: DPBS. 54
3. 0.05% trypsin-EDTA solution in DPBS. 55
4. Madin-Darby canine kidney type II (MDCK II) stable cell lines 56
cultured into 25 cm² flasks (T25, TPP) at 37 °C with 5% CO₂ 57
in humidified atmosphere expressing (*see* Fig. 2a): 58
5. E-cadherin-TSMMod: E-Cadherin tension sensor containing the 59
donor protein mTFP1 and acceptor protein EYFP separated by 60
a (GPGGA) $_8$ elastic linker [14]. 61
6. E-Cadherin-TSMMod Δ cyto: tension-less control construct of 62
the E-Cadherin tension sensor, lacking its cytoplasmic tail 63
[14] (*see* Note 1). 64
7. mTFP1-GPGGA-Venus: high FRET standard construct made 65
of mTFP1 and Venus separated by a GPGGA amino acid 66
stretch (referred to as 5aa) [17]. 67

	8. mTFP1-TRAF-Venus: low FRET standard construct made of mTFP1 and Venus separated by a 229 amino acid from Tumor Necrosis Factor Receptor Associated Factor domain (referred to as TRAF) [17].	68 69 70 71
	All cell lines and constructs are available on demand.	72 73
2.2 Cell Imaging	1. Any commercial #1.5 glass-bottomed imaging dish.	74
	2. Collagen from human placenta Bornstein and Traub Type IV (referred to as collagen) 50 µg/mL in acetic acid solution: solubilize 5 mg of collagen in 5 mL of acetic acid (0.5 M) on ice to obtain a 20× stock solution. Dilute in acetic acid (0.5 M) to obtain a solution at the final concentration of 50 µg/mL.	75 76 77 78 79
	3. Imaging medium: FluoroBrite™ DMEM (or any equivalent product), without phenol red, supplemented with 10% v/v FBS, 1% v/v PS, 2.5 mM L-Glutamine and 20 mM HEPES. Store away from light.	80 81 82 83
	4. Starvation medium: FluoroBrite™ DMEM, without phenol red, supplemented with 0.5% v/v FBS, 1% v/v PS, 2.5 mM L-Glutamine and 20 mM HEPES. Store away from light.	84 85 86
	5. Paraffin oil. Store away from the light at room temperature.	87 88
2.3 Cell Scatter Assay	1. Hepatocyte Growth Factor (HGF) 10 ng/µL in BSA/DPBS solution: solubilize 1 mg of BSA (Bovine Serum Albumin) in 1 mL of DPBS. Solubilize 10 µg of HGF in the BSA/DPBS solution. Stock as 10 µL aliquots.	89 90 91 92
	2. Stimulation medium: The day of the experiment, dilute an aliquot in 2 mL of starvation medium for a final HGF concentration of 50 ng/mL.	93 94 95 96
2.4 Wound Healing Assay	1. 200 µL pipette tips.	97
	2. Washing medium.	98 99
2.5 Microscope	1. Commercial confocal inverted microscope equipped with an incubator (37 °C and 5% CO ₂ in a humidified atmosphere).	100 101
	2. High numerical aperture immersion objectives (<i>see Note 2</i>).	102
	3. Argon laser—the 458 nm line is optimal for mTFP1 excitation—or equivalent, and a beam splitter that transmits above the excitation wavelength.	103 104 105
	4. Spectral acquisition: microscopes that use a grating in the emission path (such as Zeiss or Olympus) allow for simultaneous acquisition of the donor and acceptor emission spectra with a spectral resolution below 10 nm and nm precision (<i>see Fig. 2b, c</i>).	106 107 108 109 110 111

3 Methods		112
	Carry out all procedures in a cell culture hood unless otherwise specified.	113 114
3.1 Cell Culture Maintenance	Pass MDCK II cells three times a week as follows:	115
	1. Prepare a new cell culture flask containing 3 mL of fresh culture medium and put it into the incubator.	116 117
	2. Remove old culture medium and dead cells from the cell culture flask.	118 119
	3. Wash once with 1 mL of washing medium and by gently shaking the cell culture flask.	120 121
	4. Add 1 mL of Trypsin-EDTA solution in DPBS to the cell culture flask.	122 123
	5. Put the cell culture flask into incubator and wait about 10 min for cells to detach from the surface and from each other.	124 125
	6. Use a microscope to evaluate cell detachment.	126
	7. Once cells are detached, transfer 1:10 of the collected volume into the new flask.	127 128 129
3.2 Collagen Preparation and Coverslip Coating	1. Take glass-bottomed imaging dishes.	130
	2. Place 1 mL of collagen solution at 50 $\mu\text{g}/\text{mL}$ onto the glass-bottomed dish for 10 min at room temperature.	131 132
	3. Remove collagen solution and let dry for 1 h (<i>see Note 3</i>).	133
	4. Sterilize the dishes under UV for 20 min (<i>see Note 4</i>).	134
	5. Before use, wash the sterilized dishes with at least 1 mL of DPBS, twice.	135 136 137
3.3 Cell Seeding for Imaging	Seed cells 24 h before imaging. Prepare cells that express the tension sensor as well as cells that express the tension-less control separately. Follow steps 1–6 of the Subheading 3.1 and continue as follows:	138 139 140 141
	1. Collect the cell suspension into a sterile centrifugation tube.	142
	2. Pellet the cells by centrifugation at 60–125 $\times g$ for 5–8 min.	143
	3. Meanwhile, add culture medium onto the collagen coated imaging dishes.	144 145
	4. Discard the supernatant of the centrifugation tube and re-suspend the pellet with culture medium (<i>see Note 5</i>).	146 147
	5. Count cells with a hemacytometer or equivalent device.	148
	6. Plate 1:10 of the collected volume in a new flask with culture medium.	149 150

	7. Plate cells onto collagen coated imaging dishes: 2×10^5 for a cell scatter assay or 2×10^6 for a Wound Healing assay (<i>see Note 6</i>).	151 152 153 154
3.4 Cell Scatter Assay	1. The day after seeding, starve cells for 12 h in 2 mL imaging medium at 0.5% FBS.	155 156
	2. Wipe the bottom of the glass-bottomed dish once with optical paper and distilled water, and again with ethanol 70%.	157 158
	3. Install the imaging dish on the stage of the microscope.	159
	4. Acquire pre-treatment images (<i>see Subheading 3.6</i>).	160
	5. Replace the imaging medium with stimulation medium (<i>see Note 7</i>).	161 162
	6. Add 1 mL paraffin oil at the surface of the imaging medium to prevent evaporation (<i>see Note 8</i>).	163 164
	7. Acquire treatment images (<i>see Subheading 3.6</i>).	165
	It is recommended to perform a mock experiment in parallel by following steps 1–7 except step 5 in which the medium does not contain HGF.	166 167 168 169
3.5 Wound Healing Assay	1. The day after seeding, wash and leave cells in the washing medium for 5–10 min to loosen intercellular contacts (<i>see Note 9</i>).	170 171 172
	2. With a 200 μ L pipette tip, perform a straight scratch in the cell monolayer (<i>see Note 10</i>).	173 174
	3. Gently wash the dish with imaging medium and leave cells in 2 mL of imaging medium.	175 176
	4. Any time after the wound, wipe the bottom of the coverslip as in Subheading 3.4, step 2 and install the imaging dish on the stage of the microscope, add paraffin oil and acquire images (<i>see Subheading 3.6</i>).	177 178 179 180 181
3.6 Image Acquisition	1. Select an objective and exposure time to ensure sufficient signal to noise ratio, negligible fluorophore photobleaching and no saturation, as for standard fluorescence imaging.	182 183 184
	2. Specify multi-position settings: if desired, acquiring images from multiple positions can increase your sample size per experiment. Choose between 5–10 positions considering that the total acquisition time of each position must not exceed the duration of the time interval between frames (<i>see Note 11</i>).	185 186 187 188 189
	3. Specify Z-stack settings: if desired, this can alleviate focus drift if auto-focus is out-of-order. Make sure to avoid photobleaching.	190 191
	4. Specify time-lapse settings: cell scattering by HGF and wound healing typically occur through several hours. Choose a time interval between frames of 10 min to 1 h (<i>see Note 12</i>).	192 193 194

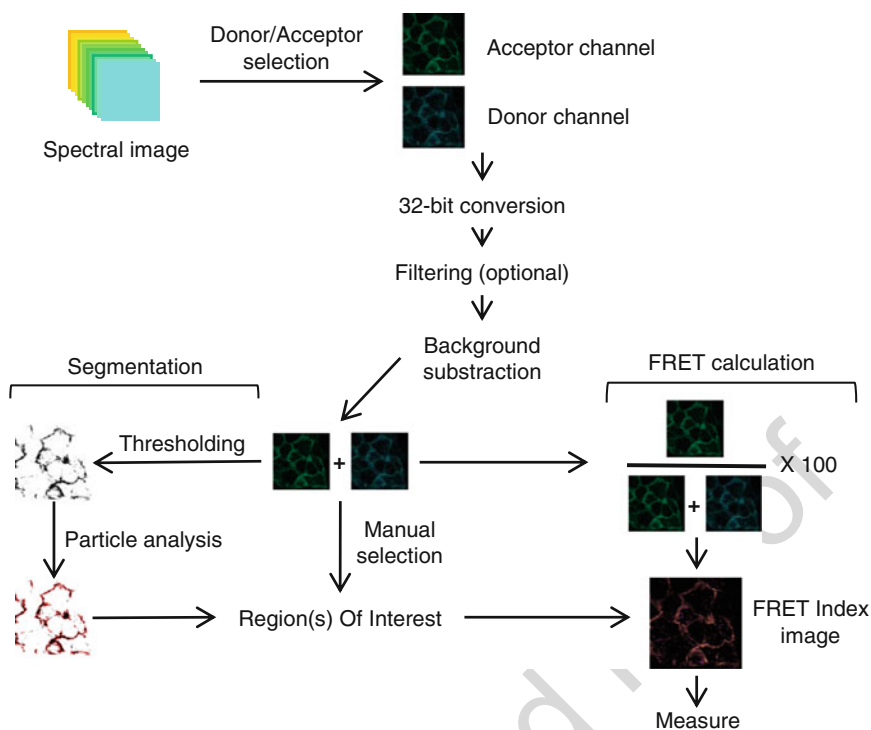


Fig. 3 Image analysis workflow for FRET calculation and image segmentation from a multi-channel spectral image

- Specify spectral acquisition settings: 10 channels in the 473–561 nm bandwidth will capture both fluorophores. This will generate a multichannel stack.

3.7 Image Analysis

Image analysis can be performed using the free and cross-platform software ImageJ, for instance its FIJI distribution (<https://fiji.sc/>) (see Fig. 3).

- Make duplicates of the raw data to avoid losses after permanent modifications (see Note 13). Generate a FRET index image as follows.
- Open an image file.
- From the multichannel stack, duplicate the donor and acceptor emission channels (D and A) that correspond to the intensity peaks of the two fluorophores (see Note 14).
- On both channels, convert image depth to 32-bit (Image>Type>32-bit).
- On both channels, subtract background: select a region devoid of cells and measure background level (Analyze>Measure), then subtract the value to the whole image (Process>Math>Subtract [Background value]) (see Note 15).

6. From both channels, generate a donor + acceptor image (D + A) that sums background corrected, donor and acceptor signals pixel by pixel. (Process>Image Calculator>Create new window>32-bit(float) result >[D] Add [A], Create a new window). 215
216
217
218
219
7. From the background corrected, acceptor channel and the sum image, generate the FRET index image A/(D + A) (Process>- Image Calculator>Create new window>32-bit(float) result> [A] Divide [D + A]). 220
221
222
223
8. Rescale the pixel values between 0 and 100. (Process>Math>Multiply [100]). 224
225
9. Select regions of interest (ROI) with any selection tool, then measure their mean gray value (Analyze>Measure) to get their FRET index. 226
227
228
10. Alternatively, ROI can be defined by segmentation based on fluorescence intensity, size and shape: select the acceptor channel (*see* **Note 16**), apply a threshold to select bright regions (Image>Adjust>Threshold, set to your taste then Apply) (*see* **Note 17**). Choose preferred bright regions according to size and shape by setting their ranges (Analyze>Analyze Particles, check Add to Manager) (*see* **Note 18**). In the ROI manager menu, save the ROI set to be able to recall it for future analyses (More>Save). Select/Open the corresponding FRET Index image (*see* Subheading 3.7, **step 7**) and click Measure in the ROI manager menu. You will obtain a measure for each ROI of the set. 229
230
231
232
233
234
235
236
237
238
239
240
241

3.8 Microscope Calibration

The FRET efficiency E can be related to the FRET index E_R computed as in 3.7 with $E = (1 - a(1 - E_R))/(1 - b(1 - E_R))$, where a and b are instrument-dependent coefficients that account for the donor's spectral bleed-through, the acceptor's direct excitation and differences in donor vs acceptor absorption cross-sections and detection efficiencies [18]. They can be recovered as follows (*see* **Note 19**): 242
243
244
245
246
247
248

1. Acquire images of the 5aa and TRAF cell lines as in Subheading 3.6. There is no need for time-lapse or Z-stack. 249
250
2. Analyze images as in Subheading 3.7. 251
3. Compute $a = (E_H(1 - E_{R,H}) - E_L(1 - E_{R,L}) + E_H E_L (E_{R,H} - E_{R,L}))/c$ and $b = (E_H(1 - E_{R,L}) - E_L(1 - E_{R,H}) + E_{R,L} - E_{R,H})/c$, with $c = (E_H - E_L)(1 - E_{R,H})(1 - E_{R,L})$, where $E_{R,H}$ and $E_{R,L}$ are the 5aa and TRAF cell lines FRET indices obtained in Subheading 3.8, **step 2**, and E_H and E_L their FRET efficiencies published elsewhere [17]. 252
253
254
255
256
257
258

3.9 Data Interpretation

1. For each experimental condition, compute the difference between the tension sensor and tension-less control FRET efficiencies (*see* **Note 20**). 259
260
261
2. Use previously published FRET efficiency to force calibration [2] to retrieve the force. 262
263
3. Mind MTM limitations in your interpretation [1]. 264
265

4 Notes

1. There exist other strategies for tension-less constructs, which may or may not give equivalent results depending on the protein of interest, as discussed in [1]. 267
268
269
2. High magnification is irrelevant but comes with high numerical aperture, which increases resolution and signal intensity, and should also come with apochromatic correction. Choose the highest you can, typically 1.4 for standard objectives. 270
271
272
273
3. Save used collagen solution back in the final concentration solution for later use. Store at 4 °C indefinitely. 274
275
4. Use the UV light of the cell culture hood. Do not cover the dishes with a plastic lid. Multiple dishes can be prepared in advance and stored on the shelf indefinitely. 276
277
278
5. When re-suspending cells, pipette up and down to shear and dissociate cell aggregates. This will facilitate homogenous seeding. 279
280
281
6. When seeding, make sure the cell suspension covers the whole coverslip by gently shaking the dish linearly in X and Y, not circularly as cells would aggregate at the center of the coverslip. 282
283
284
7. Execute with care and promptly directly on the microscope stage to keep focus, temperature and position the same. 285
286
8. Make sure there is enough oil to cover the whole surface of the imaging medium to prevent evaporation. 287
288
9. Check that the monolayer is confluent before this step. 289
10. Two perpendicular scratches maximize wound edge length per coverslip. Use/draw fiducial markers on the coverslip/imaging chamber to easily find the wound once on the microscope stage. 290
291
292
293
11. Selecting positions in close proximity minimizes the spreading and loss of the objective immersion medium. 294
295
12. Consider the total acquisition time per time-point (multiple positions and Z sections), the total duration of the time-lapse, photobleaching and phototoxicity. 20- to 30-min intervals are adequate for most experiments. 296
297
298
299

13. Name your processed files consistently with the original files but with a different name to prevent overwriting. 300
301
14. Always keep the same donor and acceptor channels throughout all your analyses. You can identify them by plotting the intensity of a region containing fluorophores against the wavelength (or channel number) (select the multichannel stack then Image>Hyperstacks>Hyperstack to Stack, then select a region and Image>Stacks>Plot Z-axis profile). The plot should display two maxima (around 490 and 530 nm), if not, do not analyze further: the cell has likely not processed the full construct properly. 302
303
304
305
306
307
308
309
310
15. Before this step, you may filter some noise by local averaging of pixel levels, at the expense of spatial resolution (for instance, Process>Filters>Gaussian Blur). 311
312
313
16. For E-cadherin-TSMod, the donor channel often exhibits intracellular aggregates, probably synthesis or degradation intermediates in which the acceptor fluorophore does not emit. Hence, the acceptor channel is preferred. 314
315
316
317
17. You can explore the different tools available on Image J to process binary images (Process>Binary>...) to improve segmentation from the thresholded image. 318
319
320
18. More information on how to use the ROI Manager tool can be found here (<https://imagej.nih.gov/ij/docs/guide/>). Size and shape selection can be very useful to exclude regions too small or round to be cell-cell contacts. In the ROI Manager, you can delete unwanted regions (>Delete) or add missing regions (draw with any selection tool then >Add). 321
322
323
324
325
326
19. This does not need to be done for every experiment but can be performed from time to time to assess the microscope stability. 327
328
20. The Ecad-TSMod Δ cyto is sensitive to intermolecular FRET [14]. This normalization thus corrects for possible FRET changes due to intermolecular FRET among other causes. 329
330
331

Acknowledgements

This work was supported in part by the Centre national de la recherche scientifique (CNRS), the French National Research Agency (ANR) grants (ANR-17-CE13-0013, ANR-17-CE09-0019, ANR-18-CE13-0008), France BioImaging infrastructure (ANR-10-INBS-04), La Ligue contre le Cancer (Allocation de recherche doctorale to HC), the European Union's Horizon 2020 research and innovation programme (Marie Skłodowska-Curie grant agreement No 665850-INSPIRE to PSC). PSC

332

333
334
335
336
337
338
339
340

acknowledges the Ecole Doctorale FIRE-Programme Bettencourt. 341
 We acknowledge the ImagoSeine facility, member of the France 342
 BioImaging infrastructure (ANR-10-INSB-04). 343

345 References

- 347 1. Gayraud C, Borghi N (2016) FRET-based 348
 349 molecular tension microscopy. *Methods* 94:33–42. [https://doi.org/10.1016/j.ymeth.](https://doi.org/10.1016/j.ymeth.2015.07.010)
 350 2015.07.010
- 351 2. Grashoff C, Hoffman BD, Brenner MD et al 352
 353 (2010) Measuring mechanical tension across
 354 vinculin reveals regulation of focal adhesion
 355 dynamics. *Nature* 466:263–266. [https://doi.](https://doi.org/10.1038/nature09198)
 356 [org/10.1038/nature09198](https://doi.org/10.1038/nature09198)
- 357 3. Meng F, Suchyna TM, Sachs F (2008) A fluo-
 358 rescence energy transfer-based mechanical
 359 stress sensor for specific proteins in situ. *FEBS*
 360 *J* 275:3072–3087. [https://doi.org/10.1111/](https://doi.org/10.1111/j.1742-4658.2008.06461.x)
 361 [j.1742-4658.2008.06461.x](https://doi.org/10.1111/j.1742-4658.2008.06461.x)
- 362 4. Ringer P, Weißl A, Cost A-L et al (2017) Multi-
 363 plexing molecular tension sensors reveals piconewton
 364 force gradient across talin-1. *Nat Methods* 14:1090–1096. [https://doi.org/10.](https://doi.org/10.1038/nmeth.4431)
 365 [1038/nmeth.4431](https://doi.org/10.1038/nmeth.4431)
- 366 5. Brenner MD, Zhou R, Conway DE et al 367
 368 (2016) Spider silk peptide is a compact, linear
 369 nanospring ideal for intracellular tension sensing. *Nano Lett* 16:2096–2102
- 370 6. Paszek MJ, DuFort CC, Rossier O et al (2014)
 371 The cancer glycocalyx mechanically primes
 372 integrin-mediated growth and survival. *Nature*
 373 511:319–325. [https://doi.org/10.1038/](https://doi.org/10.1038/nature13535)
 374 [nature13535](https://doi.org/10.1038/nature13535)
- 375 7. Zhang X, Li G, Guo Y et al (2019) Regulation
 376 of ezrin tension by S-nitrosylation mediates
 377 non-small cell lung cancer invasion and metas-
 378 tasis. *Theranostics* 9:2555–2571. [https://doi.](https://doi.org/10.7150/thno.32479)
 379 [org/10.7150/thno.32479](https://doi.org/10.7150/thno.32479)
- 380 8. Hart RG, Kota D, Li F et al (2019) Myosin II
 381 tension sensors visualize force generation
 382 within the actin cytoskeleton in living cells.
 383 *bioRxiv* 623249. [https://doi.org/10.1101/](https://doi.org/10.1101/623249)
 384 [623249](https://doi.org/10.1101/623249)
- 385 9. Suzuki A, Badger BL, Haase J et al (2016)
 386 How the kinetochore couples microtubule
 387 force and centromere stretch to move chromo-
 388 somes. *Nat Cell Biol* 18:382–392. [https://doi.](https://doi.org/10.1038/ncb3323)
 389 [org/10.1038/ncb3323](https://doi.org/10.1038/ncb3323)
- 390 10. Yamashita S, Tsuboi T, Ishinabe N et al (2016)
 391 Wide and high resolution tension
 measurement using FRET in embryo. *Sci Rep* 392
 6:28535. [https://doi.org/10.1038/](https://doi.org/10.1038/srep28535)
 393 [srep28535](https://doi.org/10.1038/srep28535) 394
- 395 11. Lagendijk AK, Gomez GA, Baek S et al (2017)
 396 Live imaging molecular changes in junctional
 397 tension upon VE-cadherin in zebrafish. *Nat*
 398 *Commun* 8:1402. [https://doi.org/10.1038/](https://doi.org/10.1038/s41467-017-01325-6)
 399 [s41467-017-01325-6](https://doi.org/10.1038/s41467-017-01325-6)
- 400 12. Lemke SB, Weidemann T, Cost A-L et al 401
 402 (2019) A small proportion of Talin molecules
 403 transmit forces at developing muscle attach-
 404 ments in vivo. *PLoS Biol* 17:e3000057.
 405 [https://doi.org/10.1371/journal.pbio.](https://doi.org/10.1371/journal.pbio.3000057)
 406 [3000057](https://doi.org/10.1371/journal.pbio.3000057)
- 407 13. Yoshida C, Takeichi M (1982) Teratocarci-
 408 noma cell adhesion: identification of a cell-
 409 surface protein involved in calcium-dependent
 cell aggregation. *Cell* 28:217–224
- 410 14. Borghi N, Sorokina M, Shcherbakova OG et al 411
 412 (2012) E-cadherin is under constitutive
 413 actomyosin-generated tension that is increased
 414 at cell-cell contacts upon externally applied
 415 stretch. *Proc Natl Acad Sci U S A* 109
 416 (31):12568–12573. [https://doi.org/10.](https://doi.org/10.1073/pnas.1204390109)
 417 [1073/pnas.1204390109](https://doi.org/10.1073/pnas.1204390109)
- 418 15. Gayraud C, Beraudin C, Déjardin T et al 419
 420 (2018) Src- and confinement-dependent FAK
 421 activation causes E-cadherin relaxation and
 422 β -catenin activity. *J Cell Biol* 217:1063–1077.
 423 <https://doi.org/10.1083/jcb.201706013>
 424 425
- 426 16. Schneider CA, Rasband WS, Eliceiri KW 427
 428 (2012) NIH image to ImageJ: 25 years of
 429 image analysis. *Nat Methods* 9:671–675.
 430 <https://doi.org/10.1038/nmeth.2089>
- 431 17. Day RN, Booker CF, Periasamy A (2008)
 432 Characterization of an improved donor fluo-
 433 rescent protein for Förster resonance energy
 434 transfer microscopy. *J Biomed Opt* 13:031203
- 435 18. Lee NK, Kapanidis AN, Wang Y et al (2005)
 436 Accurate FRET measurements within single
 437 diffusing biomolecules using alternating-laser
 438 excitation. *Biophys J* 88:2939–2953. [https://](https://doi.org/10.1529/biophysj.104.054114)
 439 doi.org/10.1529/biophysj.104.054114 440
 441 442
 443
 444